228Ra/226Ra and 226Ra/Ba ratios in the Western Mediterranean Sea: barite formation and transport in the water column

P. van Beek, E. Sternberg, J. L. Reyss, M. Souhaut, Eric Robin, C. Jeandel

$^{228}Ra/^{226}Ra$ and $^{226}Ra/Ba$ ratios in the Western Mediterranean Sea : barite formation and transport in the water column

van Beek P.[1,*], Sternberg E.[1], Reyss J.-L.[2], Souhaut M.[1], Robin E. [2], Jeandel C.[1]

[1]LEGOS, Laboratoire d'Etudes en Géophysique et Océanographie Spatiales (CNRS/CNES/IRD/UPS), Observatoire Midi Pyrénées, 14 avenue Edouard Belin, 31400 Toulouse, France
[2]LSCE, Laboratoire des Sciences du Climat et de l'Environnement (CNRS/CEA/UVSQ), 91198 Gif-sur-Yvette, France

* Corresponding author :
vanbeek@legos.obs-mip.fr
Tel. + 33 (0)5 61 33 30 51
Fax + 33 (0)5 61 25 32 05

ABSTRACT

^{226}Ra, ^{228}Ra and Ba distributions as well as $^{228}Ra/^{226}Ra$ and $^{226}Ra/Ba$ ratios were measured in seawater, suspended and sinking particles at the DYFAMED station in the Western Mediterranean Sea at different seasons of year 2003 in order to track the build-up and fate of barite through time. The study of the $^{228}Ra_{ex}/^{226}Ra_{ex}$ ratios (Ra_{ex} = Ra activities corrected for the lithogenic Ra) of suspended particles suggests that Ba_{ex} (Ba_{ex} = Ba concentrations corrected for the lithogenic Ba, mostly barite) formation takes place not only in the upper 500 m of the water column but also deeper (ie., throughout the mesopelagic layer). Temporal changes in the $^{228}Ra_{ex}/^{226}Ra_{ex}$ ratios of sinking particles collected at 1000 m depth likely reflect changes in the relative proportion of barite originating from the upper water column (with a high $^{228}Ra/^{226}Ra$ ratio) and formed in the mesopelagic layer (with a low $^{228}Ra/^{226}Ra$ ratio). $^{228}Ra_{ex}/^{226}Ra_{ex}$ ratios measured in sinking particles collected in the 1000-m trap in April and May suggest that barite predominantly formed in the upper water column during that period, while barite found outside the phytoplankton bloom period (February and June) appears to form deeper in the water column. Combining ratios of both the suspended

and sinking particles provides information on aggregation/ disaggregation processes. High $^{226}Ra_{ex}/Ba_{ex}$ ratios were also found in suspended particles collected in the upper 500 m of the water column. Because celestite is expected to be enriched in Ra (Bernstein et al., 1998), acantharian skeletons may contribute to these high ratios in shallow waters. The formation of both acantharian skeletons and barite enriched in ^{226}Ra may thus contribute to the decrease in the dissolved ^{226}Ra activity and $^{226}Ra/Ba$ ratios of surface waters observed between February and June 2003 at the DYFAMED station.

Keywords : Mediterranean Sea, barite, radium isotopes, acantharian, DYFAMED

1. INTRODUCTION

Barite ($BaSO_4$) accumulated in deep-sea sediments have been widely used for paleoceanographic studies. Because barite forms in the water column, seawater elemental distribution patterns can be recorded by authigenic barite. For instance, sedimentary barite has been used to reconstruct the paleocomposition of seawater, including strontium ($^{87}Sr/^{86}Sr$), oxygen ($^{18}O/^{16}O$) and sulfur ($^{34}S/^{32}S$) isotopic compositions (Cecile et al., 1983; Paytan et al., 1993; Martin et al., 1995; Paytan et al., 1998). Attempts to reconstruct the past Nd isotopic composition of seawater ($^{143}Nd/^{144}Nd$) have also been made (Martin et al., 1995; Paytan, 1996). Radium, a chemical analogue of barium, is also incorporated in barite and the decay of ^{226}Ra ($T_{1/2}$= 1602 y) in sedimentary barite has been used to estimate sedimentation rates and date Holocene sediment cores (Paytan et al., 1996a; van Beek and Reyss, 2001; van Beek et al., 2002; van Beek et al., 2004). In the water column, particulate Ba was shown to be mostly associated with barite (Dehairs et al., 1980, 1990, 1991; Sternberg et al., 2008). Dymond et al. (1992) proposed that excess Ba concentrations (Ba_{ex}), corresponding to the total particulate

barium concentrations corrected for the lithogenic Ba fraction, could be related solely to barite abundance. Several studies conducted either in the water column or in marine sediments have since used Ba_{ex} as a proxy of barite distribution (e.g. Shimmield et al., 1994; Gingele and Dahmke, 1994; Sternberg et al., 2008; Jacquet et al., 2008) and empirical relationships have been established between Ba_{ex} and particulate organic carbon (POC) fluxes (Dymond et al., 1992; François et al., 1995). These relationships have been used to reconstruct modern and past oceanic productivity based on the barite fluxes trapped in the water column or accumulated in the sediment, respectively (Dymond et al., 1992; Gingele and Dahmke, 1994; Shimmield et al., 1994; François et al., 1995; Paytan et al., 1996b; Nürnberg et al., 1997; Dehairs et al., 2000; Fagel et al., 2002; Fagel et al., 2004; Sternberg et al., 2007). Finally, the relationship between barite formation and the bacterial degradation of organic matter allowed several authors to use Ba_{ex} as a tool to estimate carbon remineralization rates (Dehairs et al., 1997; Cardinal et al., 2005; Jacquet et al., 2008).

Despite the wide field of applications for barite geochemistry, the mechanism of barite formation is still poorly understood. Since the world's oceans were found to be mostly undersaturated with respect to barite (Church and Wolgemuth, 1972; see also Monnin et al., 1999; Rushdi et al., 2001; Monnin and Cividini, 2006), it was proposed that barite precipitation takes place in the upper water column within supersaturated microenvironments (Chow and Goldberg, 1960). Such microenvironments could result from the decay of organic matter exported from the euphotic layer (Dehairs et al., 1980; Bishop, 1988; Stroobants et al., 1991; Dehairs et al., 1990; Dehairs et al., 1991; Dehairs et al., 1992; Ganeshram et al., 2003). The dissolution of acantharian celestite ($SrSO_4$) skeletons, enriched in barium, may also contribute to barite formation (Bernstein et al., 1987, 1992, 1998; Bernstein and Byrne, 2004). Based on observations made during the EIFEX experiment conducted in the Southern Ocean,

Jacquet et al.(2007) concluded that the dissolution of acantharian specimen could contribute to barite precipitation, but to no more than 20 % at their investigated site.

Studies conducted in the present-day ocean show that the relationship between Ba_{ex} and POC fluxes is subject to large spatial variations (Dymond et al., 1992; François et al., 1995; Sternberg et al., 2007). In particular, POC/Ba_{ex} ratios may not be the same in margin and open-ocean sites (François et al., 1995; Sanchez-Vidal et al., 2005; Sternberg et al., 2007). Among the processes that could affect the POC/Ba_{ex} relationship, one can invoke i) lateral advection that may not impact Ba_{ex} and POC distribution similarly; ii) differences in the mechanisms of barite formation between margin and open-ocean systems, including differences in the settling speeds of organic aggregates, the amount of bio-available organic matter, phytoplankton species that may favour barite precipitation etc… ; and iii) the saturation state of the ocean with respect to barite. Therefore, a better understanding of the factors controlling barite formation and transport in the water column as well as the observed spatial variation in the POC vs Ba_{ex} flux relationship is required before barite can be used with confidence as a quantitative productivity proxy.

Because Ra is a chemical analogue of Ba, Ra isotopes (^{226}Ra, $T_{1/2}$=1602 y ; ^{228}Ra, $T_{1/2}$=5.75 y) are also incorporated in Ba-rich particulate phases that form in the water column (i.e. predominantly barite and potentially acantharian skeletons enriched in Ba). Thus, radium isotopes have been shown to be powerful tracers to investigate the dynamics of barite formation and transport in the water column (Moore and Dymond, 1991 ; Legeleux and Reyss, 1996 ; van Beek et al., 2007). For instance, Moore and Dymond (1991) showed that the $^{226}Ra/Ba$ ratio in particulate matter could characterize advection of barite transported laterally from continental margins or resuspended from the seafloor by deep-sea currents. On the other hand, comparison of the $^{228}Ra/^{226}Ra$ ratio of suspended and sinking particles with seawater ratios provides useful information on the depth of barite formation in the water

column (Legeleux and Reyss, 1996) as well as on aggregation/ disaggregation processes that take place in the water column (van Beek et al., 2007). This information can be used to better constrain the key parameters that potentially control barite formation and transport in the water column (van Beek et al., 2007).

In the framework of the BARMED program (BARium in the MEDiterranean; PROOF/ INSU), we measured ^{226}Ra, ^{228}Ra and Ba distributions as well as ^{228}Ra/^{226}Ra and ^{226}Ra/Ba ratios in seawater, suspended particles and sinking particles collected at the DYFAMED station (DYnamics of Atmospheric Fluxes in the MEDiterranean Sea), in the Western Mediterranean Sea. The DYFAMED station was visited five times during year 2003 (from February to June). The main objective of this study was to track the build-up and fate of barite in relationship with the development and decay of the spring phytoplankton bloom. The determination of ^{228}Ra/^{226}Ra and ^{226}Ra/Ba ratios in both suspended and sinking particles collected at the same time allows us to provide information i) on the depth of barite formation in the water column, ii) on the transport of barite in the water column (settling to the bottom ; lateral transport ; aggregation-disaggregation processes) and iii) potentially, on the mechanisms of barite formation. This information, in turn, should be helpful to better understand the barite proxy. Additionally, very few studies have reported analyses of Ra in particulate phases. Time-series vertical profiles of both dissolved and particulate Ra activities at a given location have never been performed. Therefore, the second objective of this study was to provide information on the oceanic Ra cycle from the analysis of Ra isotopes in both dissolved and particulate phases.

2. MATERIAL and METHODS

2.1 The DYFAMED station

The DYFAMED sediment trap time-series mooring was initiated in 1988 and is located in the north-western Mediterranean Sea (43°25'N - 7°52'E) approximately 45 km south of Cape Ferrat, France, in 2,350 m of water (Fig. 1). The DYFAMED station is generally considered to be an open-ocean station (Marty et al., 2002); it is believed to be isolated from direct coastal inputs from rivers by the Liguro-provençal current but receives significant atmospheric input from the Saharan Desert (North Africa) and from industrialized countries around the Mediterranean Sea. Occasional intrusions of waters originating from the Northern Current have been observed at the DYFAMED station (Taupier-Lepage and Millot, 1986; Millot, 1999). Roy-Barman et al.(2002) recently showed that the DYFAMED station may receive significant inputs from the shelves. Sternberg et al.(2007) further reported POC/Ba_{ex} ratios in particles characteristic of a margin site. Hence, whether this station is a true open-ocean station is matter of debate.

The first study that compared the isotopic Ra signature of seawater, suspended and sinking particles was based on a single vertical profile of Ra associated with suspended particles (Sargasso Sea; van Beek et al., 2007). In the framework of the BARMED program (PROOF/ INSU), seawater samples and suspended particles were collected at the same location during five repeated visits between February and June 2003 (Table 1). Sinking particles collected during the same period in the framework of the DYFAMED sediment trap time-series were also analyzed. Repeated visits, therefore, allows us to investigate the build-up and fate of barite in relationship with the phytoplankton bloom development.

2.2 Sample Collection

Seawater samples were collected using a CTD rosette equipped with 12-liter Niskin bottles. Thirty ml of seawater were collected for dissolved Ba measurements and between 20 and 50 litres of seawater for dissolved Ra determination. Note that samples for Ba and Ra

determination were not collected within the same CTD casts. Hydrological parameters, however, show that the water column remained stable between two successive casts. Back in the laboratory, Ra isotopes were isolated by co-precipitation with a Ba carrier ($BaCO_3$ dissolved in HCl), following Schmidt and Reyss (1996). The $BaSO_4$ precipitate was recovered by decantation/ centrifugation, rinsed with 8N HCl and dried prior to analysis by gamma counting. The efficiency of Ra extraction by $BaSO_4$ precipitation was obtained by calculating the weight ratio of recovered $BaSO_4$ to introduced $BaCO_3$ (Schmidt and Reyss, 1996). The mean efficiency of the extraction protocol was 89 ± 8 %. $Ba(Ra)SO_4$ precipitates were then transferred to counting vials. Seawater samples for Ra and Ba analyses were collected during all BARMED cruises, except during BARMED #3 when stormy conditions precluded sampling large volumes of seawater for dissolved Ra analysis.

Suspended particles were collected with McLane (WTS, McLane Labs, Falmouth Ma, USA) and Challenger Oceanic (Surrey, United Kingdom) large-volume *in situ* pumps using 0.8-µm Versapor filters (acrylic copolymer on a nylon substrate; Pall Corporation) with diameters of 142 mm and 293 mm, respectively. Suspended particles were also collected by filtering small volumes of seawater collected, using Niskin bottles, through 0.45-µm polycarbonate filters. Using *in situ* pumps, suspended particles were collected with a relatively good vertical resolution during BARMED #2 (March) and #4 (May), with 7 and 10 samples collected, respectively, over the water column. Stormy conditions did not allow us to deploy *in situ* pumps during BARMED #1 (February). Only two depths could be sampled during BARMED #3 (April), again, because of bad weather conditions.

Sinking particles were collected in the framework of the DYFAMED sediment trap time-series using Technicap PPS 5 sediment traps moored at 200 and 1000 m. Analyses were conducted on dried material collected during periods associated with BARMED cruises

(integrated sampling period of 14 days). Sediment trap samples were analyzed from both the 200 m and 1000 m depth traps.

2.3 Analytical Methods

2.3.1 Seawater samples

Seawater was analyzed for barium by isotope dilution using a ^{135}Ba spike at the Inductively Coupled Plasma Mass Spectrometry (ICP-MS) facility of Observatoire Midi Pyrénées, Toulouse, France (Elan 6000 Perkin Elmer). Here we report dissolved Ba concentrations only at depths where Ra measurements were performed. More detailed Ba profiles can be found in Sternberg (2005).

Radium isotopes incorporated in the $BaSO_4$ precipitates were measured at the underground laboratory of Modane (Laboratoire Souterrain de Modane, French Alps). High-efficiency, low-background, well-type germanium detectors (215 cm^3, 430 cm^3 and 980 cm^3) were used (Reyss et al., 1995). These detectors are shielded from cosmic radiation by 1700 m of rock overburden; a very low background is thus achieved, allowing the measurement of very low activities. ^{226}Ra activities were determined using the ^{214}Pb (295 keV and 352 keV) and ^{214}Bi (609 keV) peaks. ^{228}Ra activities were determined using the 338 keV, 911 keV and 969 keV peaks of ^{228}Ac. Uncertainties reported for ^{226}Ra and ^{228}Ra activities are errors due to counting statistics (one standard deviation).

2.3.2 Particulate samples

In this study, we propose to compare the $^{228}Ra/^{226}Ra$ and $^{226}Ra/Ba$ ratios incorporated in barite ($BaSO_4$), precipitated in the water column, to the seawater ratios. Considering the small amount of barite within the suspended and sinking particles, it is not possible to separate barite from the other particles collected using *in situ* pumps or sediment traps, as it

was done with deep-sea sediment samples (Paytan et al., 1996a; van Beek et al., 2001). Consequently, particulate ratios reported here are based on bulk analyses. Total Ba and Ra concentration analyses were performed on the suspended and sinking particles. These concentrations were then corrected for the lithogenic Ba and Ra contribution in order to determine excess Ba concentrations (denoted Ba_{ex}) and excess Ra activities (denoted $^{226}Ra_{ex}$ and $^{228}Ra_{ex}$) according to :

$$Ba_{ex} = Ba_{measured} - (^{232}Th_{measured} \times [Ba/^{232}Th]_{upper\ crust}) \quad (1)$$

$$^{226}Ra_{ex} = ^{226}Ra_{measured} - (^{232}Th_{measured} \times [^{238}U /^{232}Th]_{upper\ crust}) \quad (2)$$

$$^{228}Ra_{ex} = ^{228}Ra_{measured} - (^{232}Th_{measured}) \quad (3)$$

where $Ba_{measured}$, $^{226}Ra_{measured}$ and $^{228}Ra_{measured}$ refer to the total concentrations or activities. We used the value of 51.4 (ppm/ppm) for the $[Ba/^{232}Th]_{upper\ crust}$ ratio, which is the mean ratio for the upper crust reported by Taylor and McLennan (1985). ^{226}Ra and ^{228}Ra activities were corrected for the activities in secular equilibrium with lithogenic ^{238}U and ^{232}Th, respectively. The ^{232}Th activities are entirely lithogenic. The lithogenic ^{238}U activities were estimated from the ^{232}Th activities, using the upper continental crust $^{238}U/^{232}Th$ ratio of 0.8 (dpm/dpm ; Taylor and McLennan, 1985; Anderson et al., 1990). Whereas oceanic particles may often contain an authigenic U fraction, their formation is assumed to be too recent to generate a significant ^{226}Ra ingrowth. Errors on the excess concentrations were obtained by propagating the errors of each elemental concentration (Ba, ^{226}Ra, ^{228}Ra as well as ^{232}Th). It should be stressed, however, that errors associated with the use of mean lithogenic ratios (Taylor and McLennan, 1985) to calculate the lithogenic Ba and Ra fractions may introduce errors in the calculated excess Ba and Ra concentrations.

Ra isotopes were first measured on intact filters and on dried sediment trap samples by gamma counting at the underground laboratory of Modane as described in section 2.3.1. Sediment trap material was dissolved following total digestion in a microwave oven using a

3:1 HNO_3/HF mixture. Particles on the Versapor filters were subsequently leached, in the clean laboratory, using one of the two protocols described below. Ba and ^{232}Th analyses were then conducted on the leached phases using the ICP-MS facility at Observatoire Midi Pyrénées (Elan 6000 Perkin Elmer). The dissolution of suspended particles was performed as follows:

1) A single-step leaching procedure using the method of Landing and Lewis (1991) aimed at dissolving the suspended particles was applied to about a third of the samples (Tab. 2). Following this method, filters were first subjected to a mixture of ultrapure 14N HNO_3 and 6N HCl and heated on a hot plate at 100 °C for 90 minutes. Second, ultrapure concentrated HF was added to the samples, which were placed on a hot plate for an additional 90 minutes. The filters were then rinsed with 6N HCl and removed from the solution.

2) To obtain additional information on partitioning between specific particulate phases, a slightly modified version of the five-step leaching procedure proposed by Ganeshram et al.(2003) was applied to the remaining samples (Tab. 2). Following this procedure, the filters were subjected to i) Milli-Q water; ii) dilute nitric acid (1.5N); iii) hot 1N HCl (following Weast et al., 1966); iv) hot 7.5N nitric acid; and v) total acid digestion following the protocol of Landing and Lewis (1991). These sequential leaching steps were designed to provide information on the Ba and ^{232}Th contents associated with labile organic matter (steps i and ii), barite ($BaSO_4$) (step iii), refractory organic matter (step iv) and lithogenic particles (step v). For these latter samples, the Ba leached in step iii was considered to correspond to barite (denoted Ba_{ex} in Tab. 2). For samples treated using the five-step leaching procedure, the sum of the ^{232}Th contents measured in the five leached phases was used to estimate the total ^{232}Th content in the suspended particles, which was used to correct for the ^{226}Ra and ^{228}Ra associated with the lithogenic fraction. We also compare Ba_{ex}

concentrations determined in suspended particles collected by filtering large (*in situ* pumping) and small (Niskin bottles; Sternberg et al., 2008) volumes of seawater.

Sr analyses were also performed using ICP/MS on suspended particles (small-size samples collected with Niskin bottles) leached using the single-step procedure of Landing and Lewis (1991). Sr_{ex} concentrations (excess Sr) were then determined by correcting the total Sr concentrations for the Sr associated with carbonates determined by analyzing the Ca content of the particles. The Sr content of the carbonate fraction was calculated assuming that carbonates contained 0.17 mol% Sr (Bishop et al., 1977). Previous studies have related Sr_{ex} concentrations to acantharian specimens that have a skeleton made of celestite ($SrSO_4$) (Bishop et al., 1977, 1978; van Beek et al., 2007; Jacquet et al., 2007; Dehairs et al., 2008). Acantharian specimens were observed by SEM on our filters. Acantharian skeletons dissolve readily and their sampling is difficult. Hence, quantitative sampling of acantharians typically requires the use of special preservation techniques to prevent their dissolution (see e.g. Jacquet et al., 2008). Since we did not use specific preservation protocols and a significant fraction of the acantharian skeletons likely dissolved during sampling and/ or filtration, the Sr_{ex} concentrations and the number of acantharian skeletons observed using SEM should not be considered as quantitative.

3. RESULTS

3.1 Hydrography

The vertical structure and circulation of water masses in the region has been described by Millot (1999) and references therein. CTD profiles collected on the different BARMED cruises provided information on vertical structure of water masses that was pertinent to the samples collected. Temperature, salinity, pressure and fluorescence were recorded during both downcast and upcast of the instrument. The same water masses were observed during the five

BARMED cruises. Profiles of temperature, salinity, density, fluorescence and oxygen for the five BARMED cruises can be found in Sternberg et al.(2008). Modified Atlantic Water (MAW), characterized by a subsurface salinity minimum, is found in the upper ca. 200 m of the DYFAMED water column. Just below the MAW, Levantine Intermediate Water (LIW), characterized by a salinity maximum (S=38.5) and temperature of ca. 13.5°C, is located between 200 m and 600 m. Below 1000 m depth, a fresher but colder water mass than LIW is present (Mediterranean Deep Water). Mixed layer depths found during the BARMED program ranged from 5 m to 225 m. Mixed layers were shallow during BARMED #2, #4 and #5 (25 m, 15 m, and 5 m, respectively) and much deeper during BARMED #1 (225 m; winter conditions) and BARMED #3 (160 m; stormy conditions). Stratification with warmer surface waters was well established in May and June (BARMED #4 and #5), with surface waters reaching 27.2°C in June (BARMED #5).

3.2 Phytoplankton bloom

Satellite pictures (MODIS; at http://oceancolor.gsfc.nasa.gov/cgi/level3.pl) indicate that the phytoplankton bloom started at the end of February 2003 and decreased in intensity from the end of March 2003 in the Northwestern Mediterranean Sea. This was confirmed at the DYFAMED site by POC flux measurements (Sternberg et al., 2007; Stewart et al., 2007). Fluorescence data obtained during BARMED #2 on March 23-24 also show that the phytoplankton bloom was initiated at that time. Nevertheless, depth-weighted average concentration of Chl. a during BARMED #3 on April 9-10 is higher than during BARMED #2. Sternberg et al.(2007) attributed this pattern to a short-lived bloom, also observed by Stewart et al.(2007). A secondary peak in POC flux was observed in May (Sternberg et al., 2007; Stewart et al., 2007), which Stewart et al.(2007) associated with fresh phytoplankton. These authors also identified compounds found in diatom aggregates and diatom-enriched

fecal pellets as the main constituents of material trapped in March, whereas samples recovered in early April consisted of bacterially degraded material. Therefore, BARMED #1 (mid-February) can be considered as reflecting the pre-bloom conditions. The phytoplankton bloom was clearly established during BARMED #2. The decay of the main bloom was initiated at the end of March. Thus, BARMED #3 and #4 can be associated with the decay of the main bloom, although short-lived blooms were also observed during these periods. Finally, BARMED #5 (June) represents post-bloom conditions.

3.3 Elemental Concentrations and Ratios in Seawater

^{226}Ra Activities and Ba : ^{226}Ra activities and Ba concentrations in seawater increase with depth to approximately 700 m depth, reflecting uptake during particle formation in shallow waters and subsequent release to the deep water by settling particles (Table 1; Figs. 2 and 3). Although the sampling resolution is lower below 700 m, our results suggest maximal ^{226}Ra activities at ca. 1000 m depth and slightly lower activities at greater depths. In contrast, Ba concentrations below 700 m are constant.

^{226}Ra activities measured in surface waters range from 8.1 to 10.6 dpm/ 100 l (Fig. 2). These values agree with the ^{226}Ra data reported by Schmidt and Reyss (1996) for surface waters in the same area. The single sample collected in deep waters gives a value of 9.6 dpm/ 100 l. Our data suggest that ^{226}Ra activities decrease in the upper water column from February to June (Fig. 2; see the zoom of the upper 250 m of the water column).

High resolution vertical profiles of dissolved Ba can be found in Sternberg (2005). Ba concentrations reported here range from 54.0 to 58.7 nmol l^{-1} in surface waters and reach 75.8 nmol l^{-1} in deep waters (Fig. 3). In contrast to the ^{226}Ra activities, the Ba concentrations of surface waters do not show a significant temporal variation. Using the dissolved Ba concentrations and the solubility of barite determined by Monnin et al. (2006), the barite

saturation index at the DYFAMED site was calculated (Sternberg, 2005). The calculation reveals that the entire water column is undersaturated with respect to barite, in agreement with earlier calculations reported for the Mediterranean Sea by Monnin et al.(1999).

^{228}Ra : In agreement with ^{228}Ra profiles reported from other oceanic basins, the ^{228}Ra activity profile at the DYFAMED site displays a strong vertical gradient from surface to intermediate waters (Fig. 2). Dissolved ^{228}Ra activities are highest in the upper water column and decrease rapidly through the permanent pycnocline (Moore, 1972; Kaufman et al., 1973; Li et al., 1980; Moore, 1987). The high ^{228}Ra activities in the upper water column reflect lateral transport of ^{228}Ra that diffused from shelf sediments. The low activities in intermediate waters (ca. 500-1800 m) result from the slow vertical mixing relative to radioactive decay. ^{228}Ra activities increase again close to the bottom due to diffusion from deep-sea sediments. Little temporal variation in the ^{228}Ra activities was observed during BARMED, perhaps, in part, because the error bars associated with the ^{228}Ra activities are larger than those reported for ^{226}Ra. Nevertheless, we note that surface ^{228}Ra activities were noticeably lower during BARMED #5 (June; post-bloom conditions) than during BARMED #1 (February; pre-bloom conditions).

^{226}Ra/Ba Ratio : The ^{226}Ra/Ba ratios in the water column of the DYFAMED station was found to be ca. 1.5 dpm μmol^{-1}, with a slightly lower value in deep waters (1.3 dpm μmol^{-1}; Fig. 3). The ^{226}Ra/Ba ratios measured in the upper 250 m were noticeably lower during BARMED #5 (June; post-bloom conditions) than during BARMED #1 (February; pre-bloom conditions) (see the zoom of the upper 250 m on Figure 3).

^{228}Ra/^{226}Ra Activity Ratio : The dissolved ^{228}Ra/^{226}Ra profile exhibits a gradient similar to that of the ^{228}Ra activity profile (Tab. 1). Because of the relatively small temporal variations in the ^{228}Ra/^{226}Ra ratios, all the dissolved ^{228}Ra/^{226}Ra data obtained during the

BARMED program were plotted on a single vertical profile, which allows comparison with the ratios found in particles (Fig. 4).

3.4 Elemental Concentrations and Ratios in Suspended Particles

Ba_{ex} : Ba_{ex} profiles determined from either large or small volumes of seawater (using *in situ* pumps and Niskin bottles, respectively) are similar (Fig. 4). They are generally lower in surface waters, peak in subsurface at 185-250 m depth and then decrease with increasing depths. We note, however, that Ba_{ex} concentrations determined from large volumes are systematically higher than those derived from small volumes. This is especially true for samples collected below 500 m depth. Filtration of large volumes of seawater using *in situ* pumps is expected to increase the chance to collect particles at depths where they are relatively scarce. For example, samples collected in surface waters using *in situ* pumps during BARMED #4 exhibit a very high Ba_{ex} concentration, in contrast to the sample collected with Niskin bottles (Fig. 4, panel c.). Note that the Ba_{ex} values obtained from the sequential extraction method of Ganeshram et al.(2003) are consistent with the Ba_{ex} values obtained by correcting the total Ba concentrations for the lithogenic fraction using Th as the reference lithogenic element (Fig. 4; Tab. 1). There is also a good agreement between the Ba_{ex} profiles obtained from Niskin bottle samples (particles dissolved using the one-step total dissolution method; Sternberg et al., 2008) and those obtained from *in situ* pumps (particles dissolved using either a one-step leaching method or the sequential leaching method of Ganeshram et al., 2003). These observations support the validity and efficacy of the Ganeshram et al.(2003) method.

Ba_{ex} concentrations and vertical distributions measured from BARMED #2 to BARMED #5 (Fig. 4) are similar but significantly lower concentrations were obtained during BARMED #1 (February 2003) (Sternberg et al., 2008). These latter data (obtained from

Niskin bottles) are not reported in the present paper because bad weather conditions precluded us from getting the associated particulate data with *in situ* pumps.

$^{226}Ra_{ex}$ and $^{228}Ra_{ex}$: $^{226}Ra_{ex}$ and $^{228}Ra_{ex}$ activities in suspended particles are two orders of magnitude lower than the activities in seawater. $^{226}Ra_{ex}$ and $^{228}Ra_{ex}$ activities compare well with Ba_{ex} distributions (Fig. 4). They are also generally low in surface waters, peak at 185-250 m depth and then decrease with increasing depth. Maximum values found in this study are 0.147 dpm/ 100 l for $^{226}Ra_{ex}$ during BARMED #2 in March at 185 m depth and 0.036 dpm/ 100 l for $^{228}Ra_{ex}$ during BARMED #3 in April at 100 m depth. These activities are higher than the maximum values reported in suspended particles from the Sargasso Sea, these latter values being the sole values reported up to now with which our data can be compared (0.06 dpm/ 100 l and 0.0165 dpm/ 100 l for $^{226}Ra_{ex}$ and $^{228}Ra_{ex}$, respectively; van Beek et al., 2007).

Peaks of $^{226}Ra_{ex}$ and $^{228}Ra_{ex}$ activities reach similar values during BARMED #2 (March) and #4 (May, Fig. 4; Tab. 2). Higher $^{228}Ra_{ex}$ activities were observed during BARMED #3 (April). Note that four samples were collected below 700 m during the BARMED program and only one out of these four samples showed a significant $^{228}Ra_{ex}$ activity. The $^{228}Ra_{ex}$ activity of that sample (1700 m, BARMED #4), however, is very low, being close to zero, with the result that the $^{228}Ra_{ex}/^{226}Ra_{ex}$ ratio carried a large error bar and is meaningless (Fig. 4).

$^{228}Ra_{ex}/^{226}Ra_{ex}$ Activity Ratio : $^{228}Ra_{ex}/^{226}Ra_{ex}$ activity ratios in suspended particles are generally close to the seawater ratios down to 700 m depth (Fig. 4 and Tab. 2). In most cases, the $^{228}Ra_{ex}/^{226}Ra_{ex}$ activity ratios measured below 700 m tend to zero value. Two samples collected during BARMED #3 in the upper water column, however, exhibit values significantly higher than the seawater ratios (Fig. 4). The especially high ratio found at 100 m depth during BARMED #3 (0.44; higher than the seawater ratio) can be related to the high

^{228}Ra content of these particles. We also note that the sample collected during BARMED #4 at 50 m (ie. just below the mixed layer) displays a $^{228}Ra_{ex}/^{226}Ra_{ex}$ ratio significantly lower than the seawater ratio at the same water depth, whereas slightly higher ratios than seawater are found at depth.

$^{226}Ra_{ex}/Ba_{ex}$ Ratio : $^{226}Ra_{ex}/Ba_{ex}$ ratios in suspended particles generally increase from the surface to subsurface depths (~250 m), where they reach a maximum value, higher than the seawater ratio (i.e. up to 8.4 dpm µmol^{-1}; Fig. 5). The ratios then decrease to ca. 750 m depth and remain constant below this depth. Profiles with a sufficient sampling resolution (BARMED #2 and #4) indicate that the $^{226}Ra_{ex}/Ba_{ex}$ ratios in the upper 500 m were higher during BARMED #4 (May) than during BARMED #2 (March). Ratios reported during these two cruises below 500 m depth are similar or lower than seawater ratios.

3.5 Ratios in Sinking Particles

$^{228}Ra_{ex}/^{226}Ra_{ex}$ Activity Ratio : In most cases, the $^{228}Ra_{ex}/^{226}Ra_{ex}$ activity ratio of sinking particles collected at 200 m depth is similar to that found in seawater and suspended particles collected at the same depth (Fig. 4; Tab. 3). The $^{228}Ra_{ex}/^{226}Ra_{ex}$ ratios of sinking particles collected at 1000 m depth exhibit a significant temporal variability, with ratios being either close to that found in the 200-m trap (March and April) or, when no significant $^{228}Ra_{ex}$ activities could be measured, zero (February and June). When $^{228}Ra_{ex}$ activities are measurable, the $^{228}Ra_{ex}/^{226}Ra_{ex}$ ratios range from 0.06 to 0.16, which is similar to the values reported for sinking particles in the Atlantic Ocean (Legeleux and Reyss, 1996; van Beek et al., 2007).

$^{226}Ra_{ex}/Ba_{ex}$ Ratio : $^{226}Ra_{ex}/Ba_{ex}$ ratios measured in the traps range from 1.7 to 4.8 dpm µmol^{-1} (Fig. 5; Tab 3). Whereas $^{226}Ra_{ex}/Ba_{ex}$ ratios exhibit large temporal variations in the shallow trap (2.1 to 4.8 dpm µmol^{-1}; Tab. 3), they are relatively uniform during all the

BARMED cruises in the 1000 m-trap, being ca. 2.0 dpm µmol^{-1}. For samples collected in February and March, a strong decrease in the $^{226}Ra_{ex}/Ba_{ex}$ ratio is observed between traps located at 200 m and 1000 m depth. During this period of the year, $^{226}Ra_{ex}/Ba_{ex}$ ratios in the 200 m-trap material are high (> 3.0 dpm µmol^{-1}; i.e. much higher than the seawater values reported for the same period). Similar high values were also observed in the Sargasso Sea (van Beek et al., 2007). From April to June, ratios found in the two traps are similar, with ratios remaining higher than seawater values reported in this study (ca. 2.0 dpm µmol^{-1}).

4. DISCUSSION

4.1 Ra_{ex} and Ba_{ex} Distributions in Suspended Particles and Open Questions

The occurrence of Ba_{ex} and Ra_{ex} peaks in the upper water column (i.e., above 500 m) is consistent with observations reported in previous studies and the postulate that barite precipitation takes place in the upper 500 m of the water column (Chow and Goldberg, 1960; Dehairs et al., 1980; Bishop, 1988; Dehairs et al., 1990, 1991, 1992; Legeleux and Reyss, 1996). The presence of barite among the suspended particles collected in the framework of the BARMED program was confirmed using Scanning Electron Microprobe (Fig. 5 in Sternberg et al., 2008). Quantification of the Ba associated with barite was also performed using SEM following Robin et al. (2003). The Ba_{ex} profiles obtained during the BARMED program were very similar to the barite profiles reconstructed from SEM observations (Sternberg et al., 2008). This indicates that barite is the major Ba_{ex} carrier in the water column at the DYFAMED site.

Once released from the supersaturated microenvironments in which it presumably formed, barite would settle through the water column. The relatively small barite particles may settle as a component of suspended particles, with relatively slow settling rates, or may aggregate onto larger particles that sink more rapidly. Barite could be released anytime in the

water column following the breakdown of these large particles. Transformations may also occur during settling as barite cycles through aggregation/disagreggation processes. Once released from the supersaturated microenvironments, barite may partly dissolve in undersaturated waters (Monnin et al., 1999; Monnin and Cividini, 2006). Alternatively, recrystallization may also take place during settling barite. Finally, barite may precipitate below 500 m, which would require the presence of supersaturated microenvironments at these depths (van Beek et al., 2007). Barite collected at a given depth might also have been laterally transported from more productive areas such as continental margins or resuspended from the seafloor by deep-sea currents.

Considering the different scenarios, the decreasing concentrations/activities of Ba_{ex}, $^{226}Ra_{ex}$ and $^{228}Ra_{ex}$ below 500 m (Fig. 4) could thus reflect i) a decrease in the rate at which barite is produced *in situ*, ii) gradual dissolution during settling, iii) a decrease in the supply of fine barite by breakdown of settling particles or, iv) a decrease in the supply of barite transported laterally from the margins. The $^{228}Ra_{ex}/^{226}Ra_{ex}$ and $^{226}Ra_{ex}/Ba_{ex}$ ratios can provide some insight into the relative importance of the various processes invoked above.

4.2 Origin and Fate of Ba_{ex} in the Water Column

Because the water column displays a strong vertical $^{228}Ra/^{226}Ra$ gradient, the $^{228}Ra_{ex}/^{226}Ra_{ex}$ ratio recorded by suspended and sinking particles can be used to provide information on the origin of Ba_{ex} in the water column, assuming that the $^{228}Ra_{ex}/^{226}Ra_{ex}$ ratio is predominantly determined by the Ba_{ex} component of the suspended and sinking particles (Legeleux and Reyss, 1996; van Beek et al., 2007). The $^{228}Ra_{ex}/^{226}Ra_{ex}$ ratios in suspended particles collected in the upper 700 m during BARMED #2, #5 and in most cases during BARMED #4 are close to the seawater values at the same water depth (Fig. 4). This observation is consistent with the idea that barite forms in the upper ~700 m of the water

column, as reported in previous studies (Dehairs et al., 1980; Bishop, 1988; Dehairs et al., 1990, 1991; Legeleux and Reyss, 1996; van Beek et al., 2007) and suggested by the higher Ba_{ex} and Ra_{ex} concentrations found during the BARMED program in the upper water column (Fig. 4).

The $^{228}Ra_{ex}/^{226}Ra_{ex}$ activity ratios in sinking particles display a strong temporal variability, a pattern which was also observed in other oceanic settings (Legeleux and Reyss, 1996; van Beek et al., 2007). Mass fluxes and Ba_{ex} fluxes also display large variations throughout the year (Tab. 3), but no significant correlation could be identified between the $^{228}Ra_{ex}/^{226}Ra_{ex}$ ratio of sinking particles and any of the downward fluxes (total, Ba_{ex}, organic carbon). This could in part be due to the large uncertainties in the ^{228}Ra measurements. The ballasting effect of the lithogenic, carbonate and/or Bio Si particles (François et al., 2002) may also affect the relationship between the Ba_{ex} fluxes and other mass fluxes. Ballasting and rapid sinking of particles would promote the transfer of organic carbon to the bottom but would reduce the time needed for barite to form within microenvironments of decaying organic matter (Jeandel et al., 2000; Sanchez-Vidal et al., 2005).

In most cases, the similarity between the $^{228}Ra/^{226}Ra$ ratios found at 200 m depth in sinking particles, suspended particles and seawater suggests that the 200 m-trap intercepted Ba_{ex} formed in the upper 200 m. However, we found non-significant $^{228}Ra_{ex}$ activities in the 200 m traps for BARMED #1 (February; Tab. 3) and BARMED #4 (May; Tab. 3 and Fig. 4). $^{228}Ra_{ex}/^{226}Ra_{ex}$ ratios in suspended particles collected using *in situ* pumps were also relatively low in the upper 200 m during BARMED #4. The low ratios found in the shallow trap could be explained by the presence of aged barite advected from other areas or resuspended from the continental margins.

The $^{228}Ra_{ex}/^{226}Ra_{ex}$ ratios in material recovered from the 1000 m-trap during BARMED #3 (April) and BARMED #4 (May) are significantly higher than those of

suspended particles and seawater at the same water depth. This suggests that the Ba_{ex} trapped at 1000 m depth in April and May predominantly originates from the upper water column. Cochran et al. (in press) estimated the settling speed of large particles (sinking particles) at the DYFAMED site at ca. 200 m d^{-1} during the MedFlux program that ran concurrently to the BARMED program. At such a settling rate, we do not expect a change in the $^{228}Ra_{ex}/^{226}Ra_{ex}$ ratios of the sinking particles between 200 m and 1000 m depth. In contrast, ratios tend to zero at 1000 m depth during BARMED #1 (February), BARMED #2 (March) and BARMED #5 (June). In the latter cases, the Ba_{ex} intercepted by the 1000 m trap could only originate from waters deeper than ca. 500 m, with very little contribution of Ba_{ex} from surface/ subsurface waters.

Therefore, we conclude that the Ba_{ex} intercepted by the 1000 m-trap in April and May, periods associated with the decay of the main phytoplankton bloom, seem to have been predominantly formed in shallow waters (BARMED #3 and #4). In contrast, the Ba_{ex} trapped at 1000 m depth outside the bloom period, during pre-bloom (BARMED #1) and post-bloom (BARMED #5) conditions, appears to have been produced in deeper waters. Note that even if BARMED #2 (March) corresponds to the period of phytoplankton bloom, the Ba_{ex} found in the deep trap in March does not originate from shallow waters. We expect that the Ba_{ex} formed in shallow waters during the March bloom is trapped at 1000 m depth after some lag time as it must settle from shallow waters to 1000 m depth. Alternatively, as suggested by Jeandel et al. (2000) and Sanchez-Vidal et al. (2005), ballasting and rapid sinking of particles during the early phase of the phytoplankton bloom would promote the rapid transfer of organic carbon to greater depths and may thus prevent barite from forming in shallow waters.

4.3 Lateral Transport of old Barite

Lateral transport of aged barite, possibly originating from continental margins, would have experienced significant ^{228}Ra decay and contribute to decrease the $^{228}Ra_{ex}/^{226}Ra_{ex}$ ratios of suspended and sinking particles. Lateral input of material originating from continental margins would also result in higher suspended ^{232}Th concentrations, ^{232}Th being associated with the lithogenic fraction. Finally, lateral transport of aged barite, resuspended at the margins, is expected to lower the $^{226}Ra_{ex}$ /Ba_{ex} ratio of suspended particles (Moore and Dymond, 1991).

^{232}Th concentrations at the DYFAMED station are much higher than those reported at the OFP site in the Atlantic Ocean (Fig. 6; van Beek et al., 2007). Like Ba, ^{232}Th concentrations determined from large volume filtrations are higher than those of small volume filtration below 500 m. These relatively high ^{232}Th concentrations throughout the water column suggest the presence of material of continental origin at the DYFAMED site that could consist either of Saharian dusts (eolian input; Guerzoni et al., 1997) or of lithogenic particles originating from the margins and transported into the interior by oceanic currents (Roy-Barman et al., 2002). Peaks of ^{232}Th (eg. BARMED #3, Fig. 6) suggest that lateral transport of lithogenic material cannot be excluded, especially in the upper 500 m of the water column. ^{234}Th distributions, measured during the MedFlux program in both the water column and in sediment trap material, also suggested that advection was a significant process at the DYFAMED site (Cochran et al., in press). Peaks of Ba_{ex} concentrations, however, are not always associated with a concomitant increase in ^{232}Th concentrations. Additionally, the ^{232}Th peak that developed in subsurface during BARMED #3 (Fig. 6) is not accompanied by a dramatic decrease in the $^{226}Ra_{ex}/^{228}Ra_{ex}$ ratios in suspended particles recovered at the same depth (Fig. 4), a decrease that would suggest lateral transport of aged barite. The suspended particle sample collected at 50 m during BARMED #4 also displays a low $^{226}Ra_{ex}/^{228}Ra_{ex}$ ratio that could be ascribed to the presence of aged barite transported laterally but its ^{232}Th content

is not significantly higher than samples collected just above (10 m depth) and below (112 m), samples that do not exhibit $^{226}Ra_{ex}/^{228}Ra_{ex}$ ratios lower than the seawater ratios (Fig. 4; Tab. 2). The high ^{232}Th concentrations, observed in the upper 500 m, are also not associated with low $^{226}Ra_{ex}/Ba_{ex}$ ratios. Low $^{226}Ra_{ex}/Ba_{ex}$ ratios could indicate lateral transport of old barite resuspended from the margins (Moore and Dymond, 1991). Hence, taken together, these observations suggest that the lateral transport of aged barite may not be a significant process at the DYFAMED site and likely does not affect the particulate $^{228}Ra_{ex}/^{226}Ra_{ex}$ profiles.

4.4 *In Situ* Production Versus Ageing During Settling

We can predict the $^{228}Ra_{ex}$ activity profile of suspended particles if all Ba_{ex} was produced *in situ* (i.e. at the depth of sample collection) from the $^{226}Ra_{ex}$ activities measured in suspended particles ($^{Measured}[^{226}Ra_{ex}]_z$) and the $^{228}Ra/^{226}Ra$ ratios of seawater ($^{Seawater}[^{228}Ra/^{226}Ra]_z$) at the same water depth :

$$^{Predicted}[^{228}Ra_{ex}]_z = {}^{Measured}[^{226}Ra_{ex}]_z \times {}^{Seawater}(^{228}Ra/^{226}Ra)_z \quad (4)$$

With the exception of the two high $^{228}Ra_{ex}$ activities found during BARMED #3, the predictions based on *in situ* production fall within the error bars of the data (Fig. 7), suggesting that most of the Ba_{ex} in suspension is likely produced *in situ* (i.e., at the depth of sample collection). Hence, barite precipitation may not be restricted to the upper 500 m of the water column but could also precipitate deeper in the water column (i.e., throughout the mesopelagic layer). Barite precipitation at these depths would require the presence of saturated microenvironments (ie. remineralization of organic matter or dissolving acantharian skeletons). Deep water barite formation likely explains why the $^{228}Ra_{ex}/^{226}Ra_{ex}$ ratios of the material recovered from the deep (~1000 m) sediment trap are, in some cases, lower than the ratios of particulates from the 200 m-trap (eg. BARMED #2 and #5).

On the other hand, we can predict the $^{228}Ra_{ex}/^{226}Ra_{ex}$ depth profile that would result from the settling of barite formed in subsurface waters with an initial $^{228}Ra/^{226}Ra$ ratio of 0.12 (i.e. ratio recorded by barite precipitated at 200-250 m depth, within the Ba_{ex} maximum) according to :

$$[^{228}Ra_{ex}/^{226}Ra_{ex}]_z = [^{228}Ra_{ex}/^{226}Ra_{ex}]_0 \, EXP \, (-\lambda_{228} \, z / S) \quad (5)$$

where $[^{228}Ra_{ex}/^{226}Ra_{ex}]_z$ is the $^{228}Ra_{ex}/^{226}Ra_{ex}$ ratio in suspended particles at a given water depth; $[^{228}Ra_{ex}/^{226}Ra_{ex}]_0$ is the initial $^{228}Ra/^{226}Ra$ ratio (0.12); S is the settling speed of suspended particles. $^{228}Ra_{ex}/^{226}Ra_{ex}$ profiles were generated for different settling speeds, S (Fig. 8), including the value estimated by Roy-Barman et al.(2002) (256 m a^{-1}) based on ^{230}Th data of suspended particles from the DYFAMED station. Note that this estimate is at the low end of the range of settling speeds usually reported for suspended particles (ie. 300-1000 m a^{-1}; Krishnaswami et al., 1981; Bacon and Anderson, 1982; Bacon et al., 1985). Therefore, we also generated a profile for a settling speed of 1000 m a^{-1}, what we consider to be an upper limit for the suspended particles. Note that particles may be exported faster to greater depth if they aggregate into large particles. The settling rate of large particles was estimated at ca. 200 m d^{-1} at the DYFAMED station (Cochran et al., in press; Wakeham et al., in press). At this fast settling rate, the $^{228}Ra_{ex}/^{226}Ra_{ex}$ ratios are expected to remain constant throughout the water column, a pattern that is observed in the sediment trap material collected during BARMED #3. Suspended particles may also be released at depth following disaggregation of the large particles. The release of particles originating from shallower depths is thus expected to increase the $^{228}Ra_{ex}/^{226}Ra_{ex}$ ratios of suspended particles. The $^{228}Ra_{ex}/^{226}Ra_{ex}$ ratios can thus be used to trace aggregation/ disaggregation processes when the ratios of suspended and sinking particles are compared to each other.

The best fit to the $^{228}Ra_{ex}/^{226}Ra_{ex}$ ratios observed during BARMED #2, BARMED #5 and BARMED #4 (with the exception of the ratio found at 600 m depth) requires a slow

settling velocity (approximately 40 m a^{-1}, Fig. 8). This settling speed is well below the range of values estimated from ^{230}Th data. Additionally, because the $^{228}Ra_{ex}/^{226}Ra_{ex}$ ratios of suspended particles are very close (within error bars) to the seawater ratios, this suggests that the Ba_{ex} collected below 500 m depth during these three BARMED cruises (March, May, June) likely consists of Ba_{ex} formed *in situ* (i.e., at depth of sample collection). This is especially true for samples collected during BARMED #2 (March) and BARMED #5 (June).

In contrast, the $^{228}Ra_{ex}/^{226}Ra_{ex}$ ratio of the sample collected during BARMED #4 at 600 m, being slightly higher than the seawater ratio, might be explained by Ba_{ex} originating from shallower depths (with a higher $^{228}Ra_{ex}/^{226}Ra_{ex}$ ratio) that settled with a speed of ca. 250 m a^{-1} or that was released by disaggregation of larger particles (Fig. 8). Similarly, the $^{228}Ra_{ex}/^{226}Ra_{ex}$ ratio of sample collected at 250 m in April (BARMED #3) being well above i) the seawater ratio at the same depth and ii) the prediction curves associated with the settling of suspended particles, is best explained by the disaggregation of large particles originating from shallower depths. It is difficult to explain, however, how particles assumed to form in the water column exhibit a $^{228}Ra_{ex}/^{226}Ra_{ex}$ ratio higher than the seawater ratio (i.e. sample collected during BARMED #3 at 100 m).

4.5 What Can We Learn From the ^{226}Ra/Ba Ratios ?

The ^{226}Ra/Ba ratios found in seawater at the DYFAMED station are much lower than the ratios reported in other oceanic basins (Atlantic Ocean, Pacific Ocean, Indian Ocean, Southern Ocean). The ^{226}Ra/Ba ratio was found to be very uniform within these different basins (i.e. 2.3 dpm µmol^{-1}; Chan et al., 1976; Foster et al., 2004). Low values have also been observed at the OFP site off Bermuda in the Atlantic Ocean, but only in the upper 500 m of the water column (van Beek et al., 2007). At the DYFAMED station, low ^{226}Ra/Ba ratios are found throughout the water column.

$^{226}Ra_{ex}/Ba_{ex}$ ratios in suspended particles collected in the upper ~500 m are higher than the seawater ratios but are lower than seawater ratios below this depth (Fig. 5). A similar pattern was found in the Sargasso Sea (van Beek et al., 2007). Given that Bernstein et al. (1998) predicted radium enrichments in celestite ($SrSO_4$), van Beek et al. (2007) attributed the high $^{226}Ra_{ex}/Ba_{ex}$ ratios in shallow waters to preferential uptake of ^{226}Ra over Ba into acantharian skeletons. Below 500 m depth, where few acantharian specimen remain, the lower than seawater $^{226}Ra_{ex}/Ba_{ex}$ ratios were interpreted as preferential uptake of Ba over Ra in barite formed in mesopelagic water (van Beek et al., 2007).

During BARMED #4, high Sr_{ex} concentrations (Sr corrected for the Sr associated with carbonates) were found in suspended particles in the upper ca. 150 m (Fig. 5; Sternberg, 2005). They are believed to be related to the presence of acantharian skeletons. Several acantharian specimens were observed by SEM among the suspended particles collected during the BARMED program (Fig. 9). Although these observations do not provide quantitative information, they clearly confirm the presence of acantharians and their potential influence on the Ra and Ba distributions at the DYFAMED site. The maximum $^{226}Ra_{ex}/Ba_{ex}$ ratios, however, were found at ~250 m depth at the DYFAMED site, well below the depth where acantharians are usually found (Bishop et al., 1977; 1978; Michaels, 1988; Michaels et al., 1995; Bernstein et al., 1992; Jacquet et al., 2008; Fig.5). The high $^{226}Ra_{ex}/Ba_{ex}$ ratios at depth are more likely related to barite precipitated in microenvironments with a high $^{226}Ra_{ex}/Ba_{ex}$ ratio. The dissolution of acantharian skeletons, presumably enriched in Ra, may promote the development of such microenvironments and contribute to barite precipitation. Based on the observations made during the EIFEX experiment (artificial Fe fertilization experiment) conducted in the Southern Ocean, Jacquet et al. (2007) concluded that the dissolution of acantharian skeletons could contribute to barite precipitation, but no more than 20 %. Further studies performed in natural environments that include a quantitative sampling

of acantharian skeletons should allow us to better document the relationship between acantharians, barite and the Ra cycle.

$^{226}Ra_{ex}/Ba_{ex}$ ratios in the deep and shallow traps are similar to the values reported at the OFP site, Atlantic Ocean (Fig. 5; van Beek et al., 2007). The $^{226}Ra_{ex}/Ba_{ex}$ ratios being higher than the seawater ratios suggest the presence of particles enriched in ^{226}Ra relative to Ba, which could reflect the presence of acantharian skeletons or barite precipitated following the dissolution of acantharian skeletons. $^{226}Ra_{ex}/Ba_{ex}$ ratios were especially high in the 200 m trap during BARMED #1 and #2 (Tab. 3) but remained relatively constant with time (ca. 2.0 dpm μmol^{-1}), suggesting that particles enriched in ^{226}Ra (presumably acantharian skeletons) are not preserved at depth. This observation is consistent with the distribution of these organisms within the water column : presence of acantharians as deep as 400 m has been reported but specimen become very rare to inexistent in traps located below this depth (Bernstein et al., 1992).

Finally, we note that $^{226}Ra_{ex}/Ba_{ex}$ ratios in suspended particles are higher during BARMED #4 (May) compared with BARMED #2 (March, Fig. 5). This increase in the particulate $^{226}Ra_{ex}/Ba_{ex}$ ratios parallels the decrease in the ^{226}Ra activity and $^{226}Ra/Ba$ ratios measured in seawater (Figs. 3 and 4). The ^{226}Ra decrease in surface waters is estimated at approximately 24 % while Ba concentrations do not exhibit a significant decrease. Evidence for seasonal or long-term decrease in the dissolved ^{226}Ra and/or Ba content has been reported in previous studies that related these decreases to increased primary productivity (accompanied by the removal of Ba and ^{226}Ra by barite) : Delaware Estuary (Stecher and Kogut, 1999), Black Sea (Falkner et al., 1991; Moore and Falkner, 1999). From their study conducted in the Black Sea, Falkner et al. (1991) reported a pronounced decrease in the ^{226}Ra activities and Ba concentrations of surface waters through time. Even more interesting was the observation of a decoupling between ^{226}Ra and Ba, although they are chemical analogues

(Falkner et al, 1991; Moore and Falkner, 1999). These latter studies indicate that the slight divergence in behavior of ^{226}Ra and Ba observed at the DYFAMED station may not be so surprising. The decrease in the ^{226}Ra activities and ^{226}Ra/Ba ratios of surface waters at the DYFAMED station might thus be driven by biological processes. These biological processes likely include barite precipitation and formation of acantharian skeletons that may impact both ^{226}Ra and ^{226}Ra/Ba distributions.

5. CONCLUSION

Our data indicate that barite precipitation is not restricted to the upper 500 m of the water column but can also take place deeper in the water column. These findings agree with a previous study conducted in the Sargasso Sea (van Beek et al., 2007). The collection of particles during the repeated visits of the DYFAMED station at different periods of the year suggests that the depth of barite precipitation varies seasonally in relationship with the phytoplankton bloom development. Barite intercepted at 1000 m depth in April and May, in the months following the development of the main phytoplankton bloom, mainly originates from the upper water column. In contrast, barite intercepted by the 1000 m-trap during pre-bloom and post-bloom periods mainly reflects a deep origin. This pattern may be associated with both the availability of organic matter, the depth at which its remineralization takes place in the water column and where barite precipitation is promoted. We also found evidence that barite originating from upper waters was released at depth following disaggregation of large particles. This process impacts the Ra signature of suspended particles.

High $^{226}Ra_{ex}/Ba_{ex}$ ratios (i.e. much higher than the seawater ratios) were found in suspended and sinking particles collected in the upper 500 m of the water column. Such high ratios are not found deeper in the water column and suggest that Ra enrichment is associated

with particles that are not preserved at depth. These high $^{226}Ra_{ex}/Ba_{ex}$ ratios may constitute a signature of acantharian skeletons and barite that precipitated following the dissolution of celestite skeletons. These particles, enriched in ^{226}Ra, may thus contribute significantly to the ^{226}Ra and $^{226}Ra/Ba$ decreases observed in surface waters from February to June at the DYFAMED station. Further studies conducted in natural environments, including a quantitative sampling of acantharian skeletons, should allow us to better document the relationship between acantharians, barite and the ^{226}Ra cycle.

Acknowledgments :

We are grateful to Captain and Crew of R.V. Téthys II. We thank Claudie Marec and Christophe Guillerm (DT INSU) for their assistance at sea. We thank Aurélien Rojas at the underground laboratory of Modane (LSM, France) and Frédéric Candaudap at the ICP-MS facility of the Observatoire Midi Pyrénées, Toulouse, France. Time-series sediment trap samples were obtained in the framework of the "Service d'Observation DYFAMED" supported by France-INSU. This work was supported by the French program PROOF (biogeochemical PROcesses in the Ocean and Fluxes). We thank Stéphanie Jacquet, Kirk Cochran and two anonymous reviewers for their constructive reviews that allowed us to improve significantly the quality of the manuscript. We are especially grateful to A. Mucci, Associate Editor of GCA, for his careful and constructive editorial review.

REFERENCES

Anderson, R.F., Lao, Y., Broecker, W.S., Trumbore, S.E., Hofman, H.J., Wolfli, W., 1990. Boundary scavenging in the Pacific Ocean : a comparison of ^{10}Be and ^{231}Pa. *Earth Planet. Sci. Lett*. 96, 287-304.

Bacon, M.P., Anderson, R. F., 1982. Distribution of thorium isotopes between dissolved and particulate forms in the deep sea. *Journal of Geophys. Res.* 87, 2045-2056.

Bacon, M.P., Huh, C.-A., Fleer, A.P., Deuser, W.G., 1985. Seasonality in the flux of natural radionuclides and plutonium in the deep Sargasso Sea. *Deep-Sea Res. I* 32 (3), 273-286.

Bernstein, R.E., Betzer, P.R., Feely, R.A., Byrne, R.H., Lamb, M.F., Michaels, A.F., 1987. Acantharian fluxes and strontium to chlorinity ratios in the North Pacific Ocean. *Science* 237, 1490-1494.

Bernstein, R.E., Byrne, R.H., Betzer, P.R., Greco, A.M., 1992. Morphologies and transformations of celestite in seawater : the role of acantharians in strontium and barium geochemistry. *Geochim. Cosmochim. Acta* 56, 3273-3279.

Bernstein, R.E., Byrne, R.H., Schijf, J., 1998. Acantharians : a missing link in the oceanic biogeochemistry of barium. *Deep-Sea Res. II* 45, 491-505.

Bernstein, R.E., Byrne, R.H., 2004. Acantharians and marine barite. *Mar. Chem.* 86, 45-50.

Bishop, J.K.B., Edmond, J.M., Ketten, D.R., Bacon, M.P., Silker, W.B., 1977. The chemistry, biology, and vertical flux of particulate matter from the upper 400 m of the equatorial Atlantic Ocean. *Deep-Sea Res.* 24, 511-548.

Bishop, J.K.B., Ketten, D. R., Edmond, J.M., 1978. The chemistry, biology, and vertical flux of particulate matter from the upper 400 m of the Cape Basin in the southeast Atlantic Ocean. *Deep-Sea Res.* 25, 1121-1161.

Bishop, J.K.B., 1988. The barite-opal-organic carbon association in oceanic particulate matter. *Nature* 332, 341-343.

Cardinal, D., Savoye, N., Trull, T.W., André, L., Kopczynska, E.E., Dehairs, F., 2005. Variations in the Southern Ocean illustrated by the Ba_{ex} proxy. *Deep-Sea Res.* 52, 355-370.

Cecile, M.P., Shaker, M.A., Krause, H.R., 1983. The isotopic composition of western Canadian barites and the possible derivation of oceanic sulfate $\delta^{34}S$ and $\delta^{18}O$ age curve, *Can. J. Earth Sci*. 20, 1528-1535.

Chan, L.H., Edmond, J.M., Stallard, R.F., Broecker, W.S., Chung., Y.C., Weiss R.F., Ku, T.L., 1976. Radium and barium at GEOSECS stations in the Atlantic and Pacific. *Earth Planet. Sci. Lett.* 32, 258-267.

Chow, T.J., Goldberg, E.D., 1960. On the marine geochemistry of barium. *Geochim. Cosmochim. Acta* 20, 192-198.

Church, T.M., Wolgemuth, K., 1972. Marine barite saturation. *Earth Planet. Sci. Lett.* 15, 35-44.

Cochran, K.J., Miquel, J.C., Armstrong, R., Fowler, S.W., Masqué, P., Gasser, B., Hirschberg, B., Szlosek, J., Rodriguez y Baena, A.M., Verdeny, E., Stewart, G.M., Time-series measurements of ^{234}Th in water column and sediment trap samples from the northwestern Mediterranean Sea, *Deep-Sea Res.* in press.

Dehairs, F., Chesselet, R., Jedwab, J., 1980. Discrete suspended particles of barite and the barium cycle in the open ocean. *Earth Planet. Sci. Lett.* 49, 528-550.

Dehairs, F., Goeyens, L., Stroobants, N., Bernard, P., Goyet, C., Poisson, A., Chesselet, R., 1990. On suspended barite and the oxygen minimum in the Southern Ocean. *Global Biogeochem. Cycles* 4 (1), 85-102.

Dehairs, F., Stroobants, N., Goeyens, L., 1991. Suspended barite as tracer of biological activity in the Southern Ocean. *Mar. Chem.* 35, 399-410.

Dehairs F., Baeyens W. and Goeyens, L., 1992. Accumulation of suspended barite at mesopelagic depths and export production in the Southern Ocean. *Science* 258, 1332-1335.

Dehairs, F., Shopova, D., Ober, S., Veth, C., Goeyens, L., 1997. Particulate barium stocks and oxygen consumption in the Southern Ocean mesopelagic water column during spring and early summer : relationship with export production. *Deep-Sea Res.* 44, 497-516.

Dehairs, F., Fagel., N., Antia, A.N., Peinert, R., Elskens, M., Goeyens, L., 2000. Export production in the Bay of Biscay as estimated from barium-barite in settling material : a comparison with new production. *Deep-Sea Res. I* 47, 583-601.

Dehairs, F., Jacquet, S., Savoye, N., van Mooy, B.A.S., Buesseler, K.O., Bishop, J.K.B., Lamborg, C.H., Elskens, M., Baeyens, W., Boyd, P.W., Casciotti, K.L., Monnin, C., 2008. Barium in the twilight suspended matter as potential proxy for particulate organic carbon remineralization : Results for the North Pacific. *Deep-Sea Res.* 55, 1673-1683.

Dymond J., Suess E. and Lyle M., 1992. Barium in deep-sea sediment : A geochemical proxy for paleoproductivity. *Paleoceanography* 7 (2), 163-181.

Fagel, N., Dehairs, F., André, L., Bareille, G. and Monnin, C. (2002). Ba distribution in surface Southern Ocean sediments and export production estimates, *Paleoceanography* 17, 1-21.

Fagel, N., Dehairs, F., Peinert, R., Antia, A., André, L., 2004. Reconstructing export production at the NE Atlantic margin : potential and limits of the Ba proxy, *Marine Geology* 204, 11-25.

Falkner, K.K., D.J. O'Neill, J.F. Todd, W.S. Moore, J.M. Edmond, 1991. Depletion of barium and radium-226 in Black sea surface waters over the past thirty years, *Nature* 350, 491-494.

Foster, D.A., Staubwasser, M., Henderson, G.M., 2004. ^{226}Ra and Ba concentrations in the Ross Sea measured with multicollector ICP mass spectrometry. *Mar. Chem.* 87, 59-71.

François, R., Honjo, S., Manganini, S.J., Ravizza, G.E., 1995. Biogenic barium fluxes to the deep sea : Implications for paleoproductivity reconstruction. *Global Biogeochem. Cycles* 9 (2), 289-303.

François, R., Honjo, S., Krishfield, R., Manganini, S., 2002. Factors controlling the flux of organic carbon to the bathypelagic zone of the ocean. Global Biogeochemical Cycles 16, 1087 (16, 1087, doi:10.1029/2001GB001722).

Ganeshram, R.S., François, R., Commeau, J., Brown-Leger, S.L., 2003. An experimental investigation of barite formation in seawater. *Geochim. Cosmochim. Acta.* 67 (14), 2599-2605.

Gingele, F., Dahmke A., 1994. Discrete barite particles and barium as tracers of paleoproductivity in South Atlantic sediments. *Paleoceanography* 9 (1), 151-168.

Guerzoni, S., Molinaroni, E., Chester, R., 1997. Saharian dust inputs to the western Mediterranean Sea : depositional patterns, geochemistry and sedimentological implications. *Deep-Sea Res.* II, 44, 631-654.

Jacquet, S.H.M., Henjes, J., Dehairs, F., Worobiec, A., Savoye, N., Cardinal, D., 2007. Particulate Ba-barite and acantharians in the Southern Ocean during the European Iron Fertilization Experiment (EIFEX), *Journal of geophys. Res.*112, G04006, doi:10.1029/2006JG000394.

Jacquet, S.H.M., Dehairs, F., Savoye, N., Obernosterer, I., Christaki, U., Monnin, C., Cardinal, D., 2008. Mesopelagic organic carbon remineralization in the Kerguelen Plateau region tracked by biogenic particulate Ba., *Deep-Sea Res.* 55, 868-879.

Jeandel, C., Tachikawa, K., Bory, A., Dehairs, F., 2000. Biogenic barium in suspended and trapped material as a tracer of export production in the tropical NE Atlantic EUMELI sites, Mar. Chem. 71, 125–142.

Kaufman, A., Trier, R.M., Broecker, W.S., Feely, H.W., 1973. Distribution of ^{228}Ra in the world ocean. *Journal of geophys. Res.* 78 (36), 8827-8848.

Krishnaswami, S., Sarin, M.M., Somayajulu, B.L.K., 1981. Chemical and radiochemical investigations of surface and deep particles in the Indian Ocean. *Earth Planet. Sci. Lett.* 54, 81-96.

Landing, W.M., Lewis, B.L., 1991. Collection, processing, and analysis of marine particulate and colloidal material for transition metals. In : Spencer, D.C.H.a.D.W. (Ed), Marine Particles: Analysis and Characterization, vol. 63. Geophysical Monograph, Washington, DC, pp. 263-27.

Legeleux, F., Reyss, J.-L., 1996. Ra-228/ Ra-226 activity ratio in oceanic settling particles : Implications regarding the use of barium as a proxy for paleoproductivity reconstruction. *Deep-Sea Res. I* 43 (11-12), 1857-1863.

Li, Y.-H., Feely, H. W., Toggweiler, J.R., 1980. ^{228}Ra and ^{228}Th concentrations in GEOSECS Atlantic surface waters, *Deep-Sea Res.* 27A, 545-555.

Martin, E.E., Macdougall, J.D., Herbert, T.D., Paytan, A., Kastner, M., 1995. Strontium and neodymium isotopic analyses of marine barite separates, *Geochim. Cosmochim. Acta* 59 (7), 1353-1361.

Marty, J.-C., Chiavérini, J., Pizay, M.-D., Avril, B., 2002. Seasonal and interannual dynamics of nutrients and phytoplankton pigments in the western Mediterranean Sea at the DYFAMED Time-series station (1991-1999). *Deep-Sea Res.* II, 49, 1965-1985.

Michaels, A.F., 1988. Vertical distribution and abundance of Acantharia and their symbionts. *Marine Biology* 97, 559-569.

Michaels, A.F., Caron, D.A., Swanberg, N.R., Howse F.A., Michaels, C., 1995. Planktonic sarcodines (Acantharia, Radiolaria, Foraminifera) in surface waters near Bermuda : abundance, biomass and vertical flux. *Journal of Plankton Res.* 17 (1), 131-163.

Millot, C., 1999. Circulation in the Western Mediterranean Sea, *Journal of Marine Systems* 20 (1-4), 423-442.

Monnin, C., Jeandel, C., Cattaldo, T., Dehairs F., 1999. The marine barite saturation state of the world's oceans. *Mar. Chem.* 65, 253-261.

Monnin, C., Cividini, D., 2006. The saturation state of the world's ocean with (Ba,Sr)SO4 solid solutions. *Geochim. Cosmochim. Acta* 70, 3290-3298.

Moore W.S., 1972. Radium-228 : application to thermocline studies, *Earth Planet. Sci. Lett.* 16, 421-422.

Moore, W.S., 1987. Radium 228 in the South Atlantic Bight. *Journal of geophys. Res.* 92, 5177-5190.

Moore, W.S., Dymond J., 1991. Fluxes of Ra-226 and barium in the Pacific Ocean : The importance of boundary processes. *Earth Planet. Sci. Lett.* 107, 55-68.

Moore, W.S., Falkner, K.K., 1999. Cycling of radium and barium in the Black Sea, *Journal of Environmental Radioactivity* 43, 247-254.

Nürnberg, C.C., Bohrmann, G., Schlüter, M., 1997. Barium accumulation in the Atlantic sector of the Southern Ocean : Results from 190,000-year records. *Paleoceanography* 12 (4), 594-603.

Paytan, A., Kastner, M., Martin, E.E., Macdougall, J.D., and Herbert, T., 1993. Marine barite as a monitor of seawater strontium isotope composition, *Nature* 366, 45-49.

Paytan, A., Moore W.S., Kastner, M., 1996a. Sedimentation rate as determined by ^{226}Ra activity in marine barite. *Geochim. Cosmochim. Acta* 60 (22), 4313-4319.

Paytan, A., Kastner, M., Chavez, F.P., 1996b. Glacial to Interglacial fluctuations in productivity in the equatorial Pacific as indicated by marine barite. *Science* 274, 1355-1357.

Paytan, A., 1996. Marine barite : a recorder of oceanic chemistry, productivity and circulation. PhD Thesis. University of California, San Diego. 111pp.

Paytan, A., Kastner, M., Campbell, D., Thiemens, M.H., 1998. Sulfur isotopic composition of cenozoic seawater sulfate, *Science* 282, 1459-1462.

Reyss, J.-L., Schmidt, S., Legeleux, F., Bonte, P., 1995. Large, low background well-type detectors for measurements of environmental radioactivity. *Nucl. Inst. and Meth. A* 357, 391-397.

Robin, E., Rabouille, C., Martinez, G., Lefevre, I., Reyss, J.-L., van Beek, P., Jeandel, C., 2003. Direct bio-Ba determination using SEM/EDS-ACC system : implication for barite preservation in marine sediments, *Mar. Chem.* 82 (3-4), 289-306.

Roy-Barman, M., Coppola, L., Souhaut, M., 2002. Thorium isotopes in the western Mediterranean Sea : an insight into the marine particle dynamics, *Earth Planet. Sci. Lett.*196, 161-174.

Rushdi, A., McManus, J., Collier., R., 2000. Marine barite and celestite saturation in seawater. *Mar. Chem.* 69, 19-31.

Sanchez-Vidal, A., Collier, R.W., Calafat, A., Fabres, J., Canals, M., 2005. Particulate barium fluxes on the continental margin : a study from the Alboran Sea (western Mediterranean), *Mar. Chem.* 93, 105-117.

Schmidt, S., Reyss, J.-L., 1996. Radium as internal tracer of Mediterranean outflow water. *Journal of Geophys. Res.* 101, 3589-3596.

Shimmield, G., Derrick, S., Mackensen, A., Grobe, H., Pudsey, C., 1994. The history of barium, biogenic silica and organic carbon accumulation in the Weddell Sea and Antarctic Ocean over the last 150,000 a, *in* : Zahn *et al.* (ed.), *Carbon Cycling in the Glacial Ocean : Constraints on the Ocean's Role in Global Change*, NATO ASI Series I 17, 555-574, Springer-Verlag, Berlin.

Stecher, H.A., Kogut, M. B., 1999. Rapid barium removal in the Delaware estuary, *Geochim. Cosmochim.* Acta 63, 1003-1012.

Sternberg, E., 2005. La barytine, quel traceur en océanographie ? PhD. Thesis, LEGOS, Observatoire Midi Pyrénées, Toulouse, France, 260 pp.

Sternberg, E., Miquel, J.C., Gasser, B., Souhaut, M., Arraes-Mescoff, R., Jeandel, C. and François, R., 2007. Barium fluxes and export production in the northwestern Mediterranean, *Mar. Chem.* 105, 281-295.

Sternberg, E., Robin, E., Souhaut, M. and Jeandel C., 2008. Seasonal cycle of suspended barite in the Mediterranean Sea, Geochimica Cosmochimica Acta 72, 4020-4034.

Stewart, G., Cochran, J.K., Xue, J., Lee, C., Wakeham, S.G., Armstrong, R.A. Masqué, P., 2007. Exploring the use of ^{210}Po as a tracer of organic matter flux in the northwestern Mediterranean. *Deep-Sea Research* I, 54, 415-427.

Stroobants, N., Dehairs, F., Goeyens, L., Vanderheijden, N., van Grieken, R., 1991. Barite formation in the Southern Ocean water column. *Mar. Chem.* 35, 411-421.

Taupier-Letage, I., Millot, C., 1986. General hydrodynamical features in the Ligurian Sea inferred from the DYOME experiment, *Oceanologica Acta* 9 (2), 119-131.

Taylor, S.R., McLennan, S.M., 1985. The continental crust : its composition and evolution, Blackwell, Cambridge, Massachusetts.

van Beek, P., Reyss, J.-L., 2001. ^{226}Ra in marine barite : new constraints on supported ^{226}Ra. *Earth Planet. Sci. Lett.* 187, 147-161.

van Beek, P., Reyss, J.-L., Gersonde, R., Paterne, M., Rutgers van der Loeff, M., Kuhn, G., 2002. ^{226}Ra in barite : absolute dating of Holocene Southern Ocean sediments and reconstruction of sea-surface reservoir ages. *Geology* 30 (8), 731-734.

van Beek, P., Reyss, J-L., DeMaster, D., Paterne, M., 2004. ^{226}Ra-in marine barite : Relationship with carbonate dissolution and sediment focusing in the equatorial Pacific. *Deep-Sea Research I* 51, 235-261.

van Beek, P., François, R., Conte, M., Reyss J.-L., Souhaut, M., Charette, M., 2007. ^{228}Ra/^{226}Ra and ^{226}Ra/Ba ratios to track barite formation and transport in the water column, *Geochim. Cosmochim. Acta* 71, 71-86.

Wakeham, S.G., Lee, C., Peterson, M.L., Liu, Z., Szlosek, J., Putman, I.F., Xue, J. Organic biomarkers in the twilight zone - time series and settling velocity sediment traps during MedFlux, *Deep-Sea Res.* in press.

Weast, R.C., Selby, S.M., Hodgman, C.D., 1966. Handbook of chemistry and physics, 46th edition, the chemical rubber co., Cleveland, 1713 pp.

Table 1 : Radium and barium analyses conducted on the dissolved phase.

Table 2 : Measurements conducted on suspended particles.

Table 3 : Measurements conducted on sinking particles.

(See Table file)

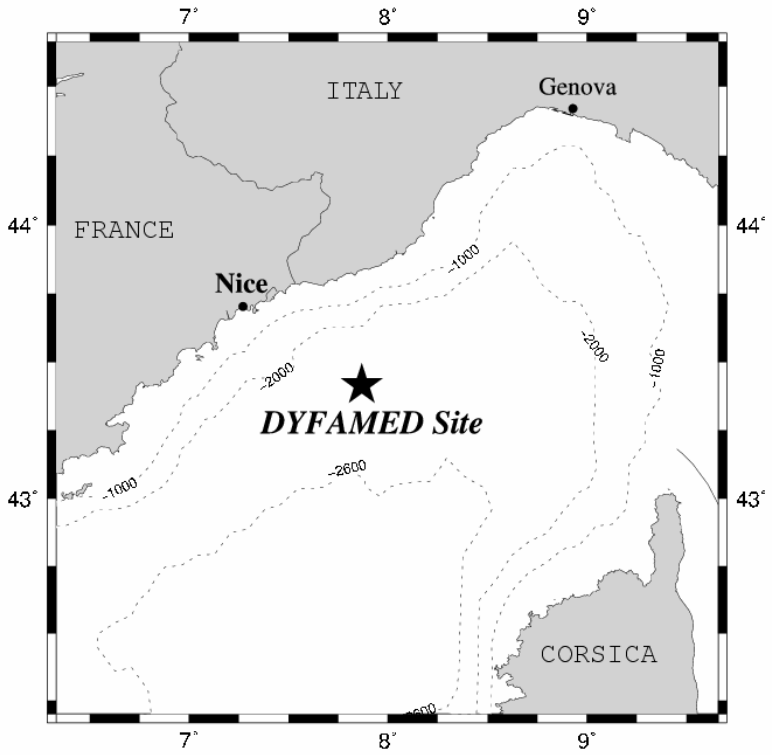

Figure 1 : Location of the DYFAMED station investigated during the BARMED program (Western Mediterranean Sea).

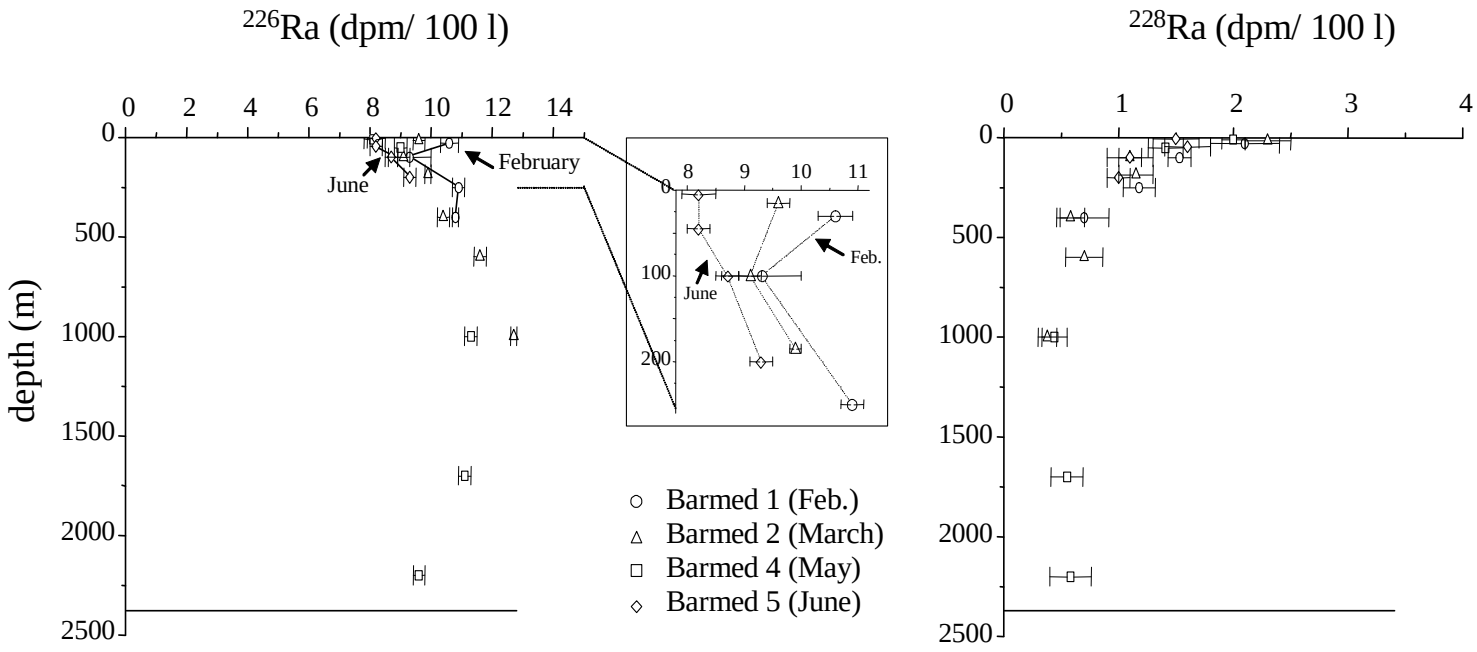

Figure 2 : ^{226}Ra and ^{228}Ra activities in the dissolved phase. A zoom of the upper 250 m of the water column is shown for the ^{226}Ra activities. For clarity, we did not report all the data on the latter plot. The lower horizontal lines denote the depth of the bottom.

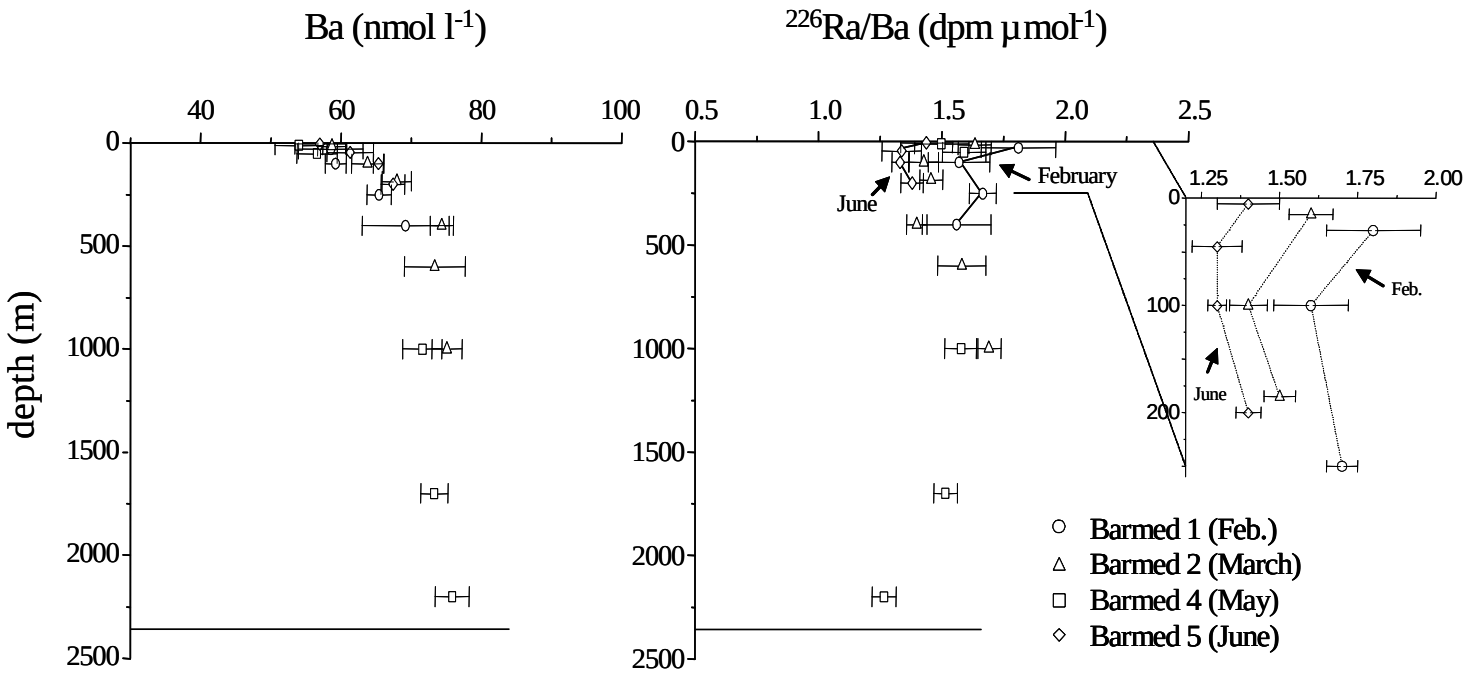

Figure 3 : Ba concentrations and ^{226}Ra/Ba ratios in the dissolved phase. A zoom of the upper 250 m of the water column is shown for the ^{226}Ra/Ba ratios. For clarity, we did not report all the data on the latter plot. The lower horizontal lines denote the depth of the bottom.

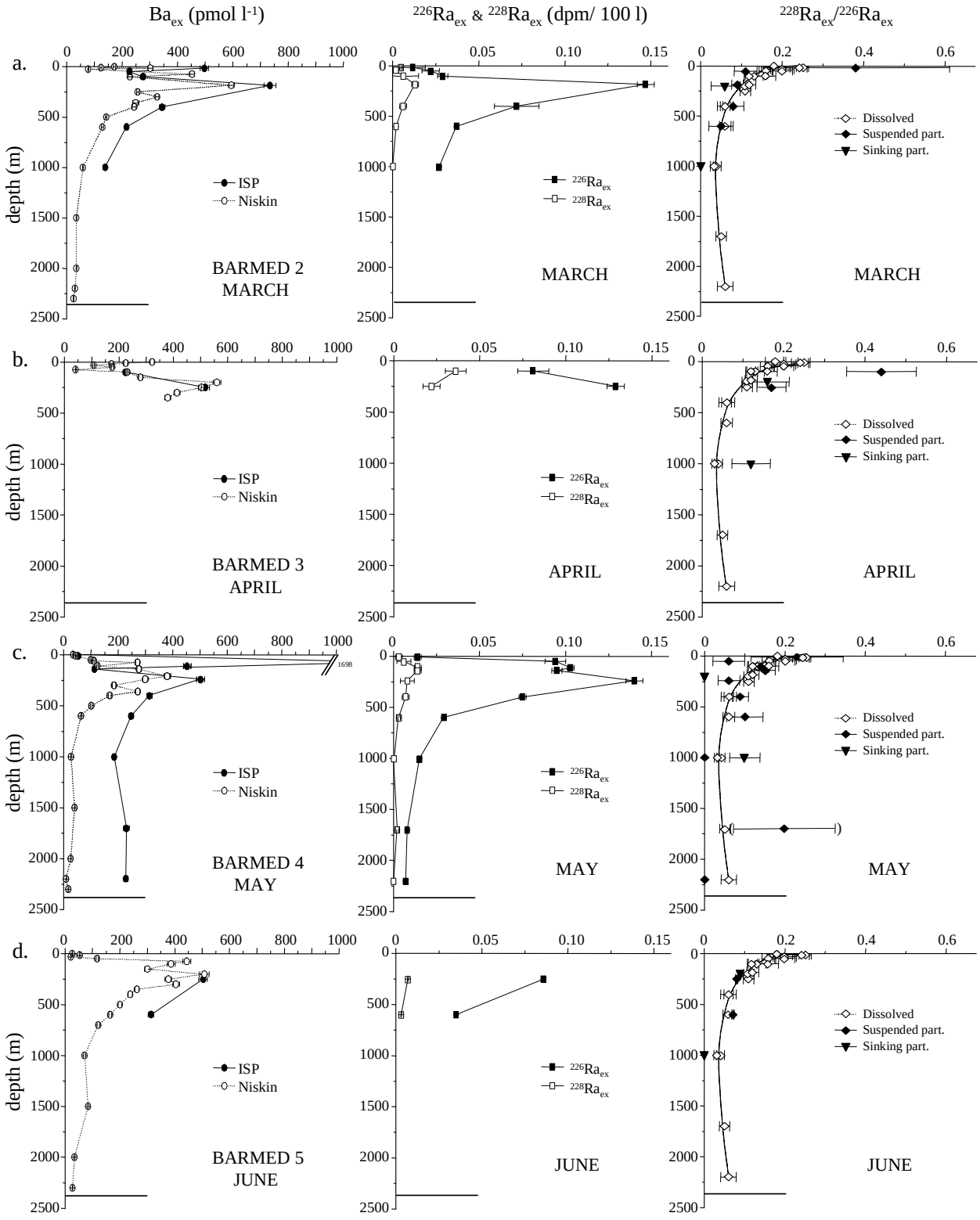

Figure 4 : Excess Ba concentrations, ^{226}Ra and ^{228}Ra activities (Ba_{ex}, $^{226}Ra_{ex}$ and $^{228}Ra_{ex}$) measured in the suspended particles (panels a to d : BARMED 2 to 5). Ba_{ex} concentrations are reported for samples collected using either *in situ* pumps (denoted ISP) or Niskin bottles (denoted Niskin). $^{228}Ra/^{226}Ra$ ratios in both suspended and sinking particles are compared to the seawater ratios. The line in the right figures is the seawater $^{228}Ra/^{226}Ra$ profile.

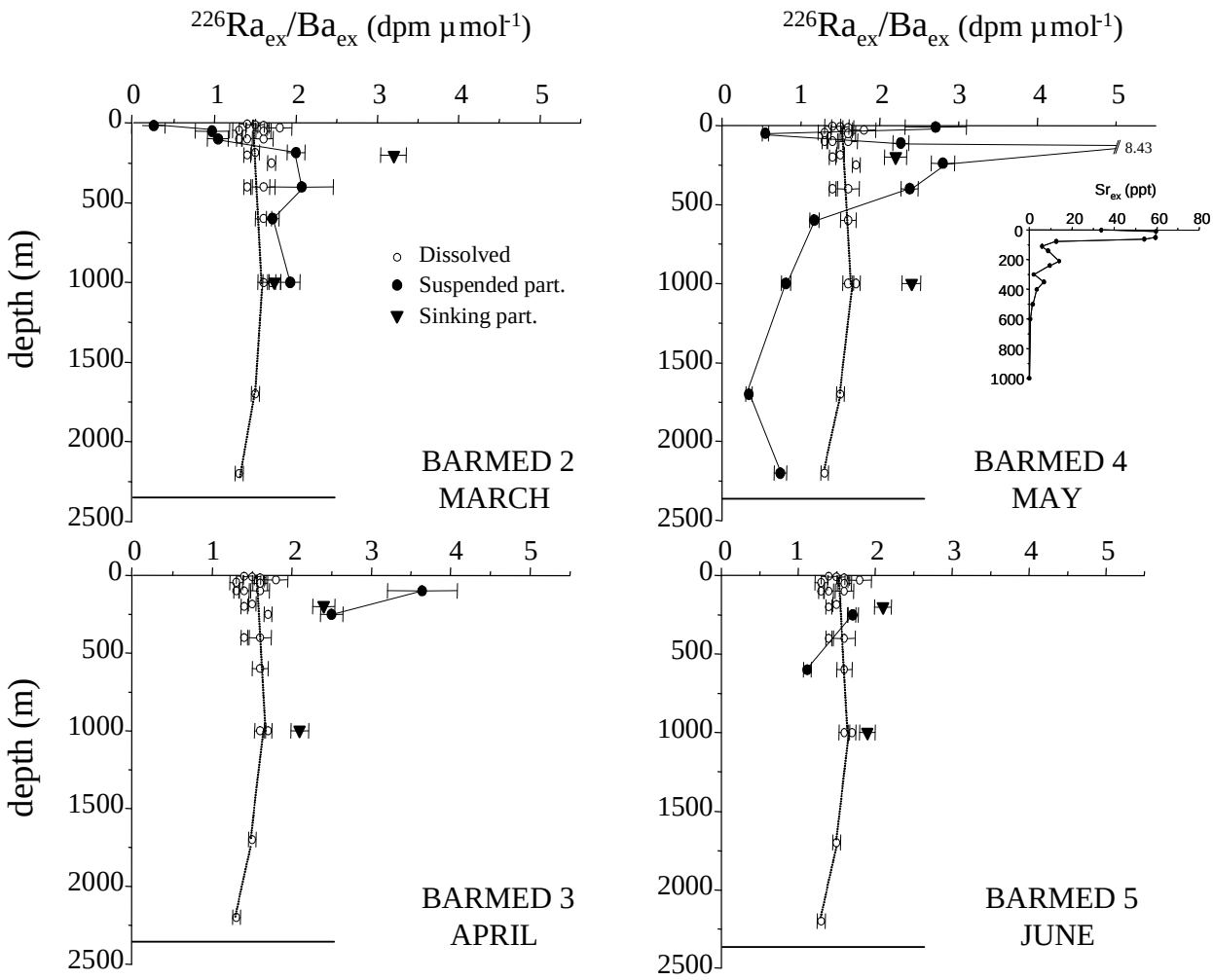

Figure 5 : $^{226}Ra_{ex}/Ba_{ex}$ ratios of both suspended and sinking particles compared with the seawater $^{226}Ra/Ba$ ratios (BARMED 2 to BARMED 5). The seawater $^{226}Ra/Ba$ ratios reported on each plot include all the data from the BARMED program. In contrast, the $^{226}Ra_{ex}/Ba_{ex}$ ratios of suspended and sinking particles were obtained from individual BARMED cruises. The particulate Sr_{ex} concentrations (total Sr corrected for Sr associated with carbonates) measured during BARMED 4 are also reported ; the Sr_{ex} concentrations are believed to be related to the Sr associated with acantharians (Bishop et al., 1977, 1978). These latter samples were collected with Niskin bottles (filtration of small volumes of seawater).

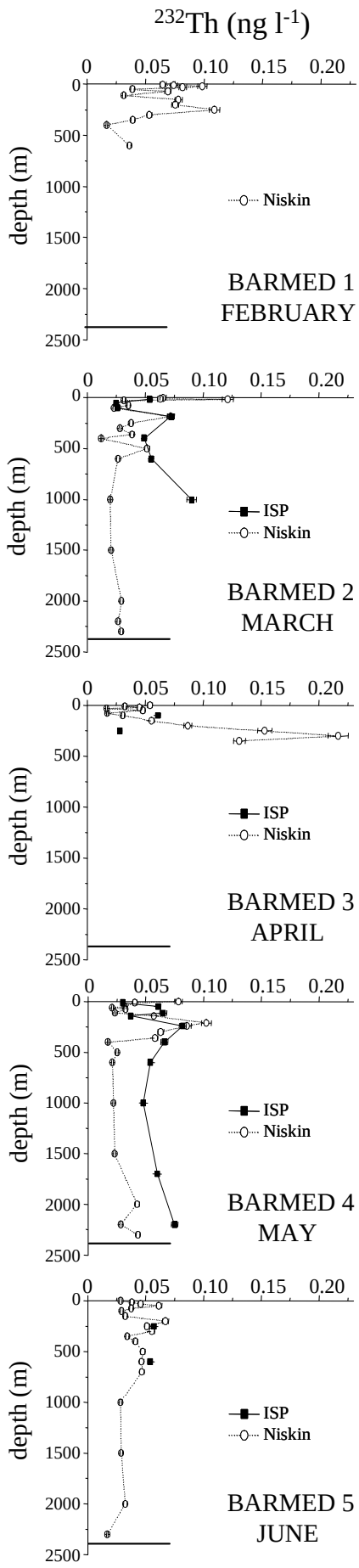

Figure 6 : ^{232}Th concentrations in suspended particles collected using *in situ* pumps (denoted ISP; large volume) and Niskin bottles (denoted Niskin; small volume).

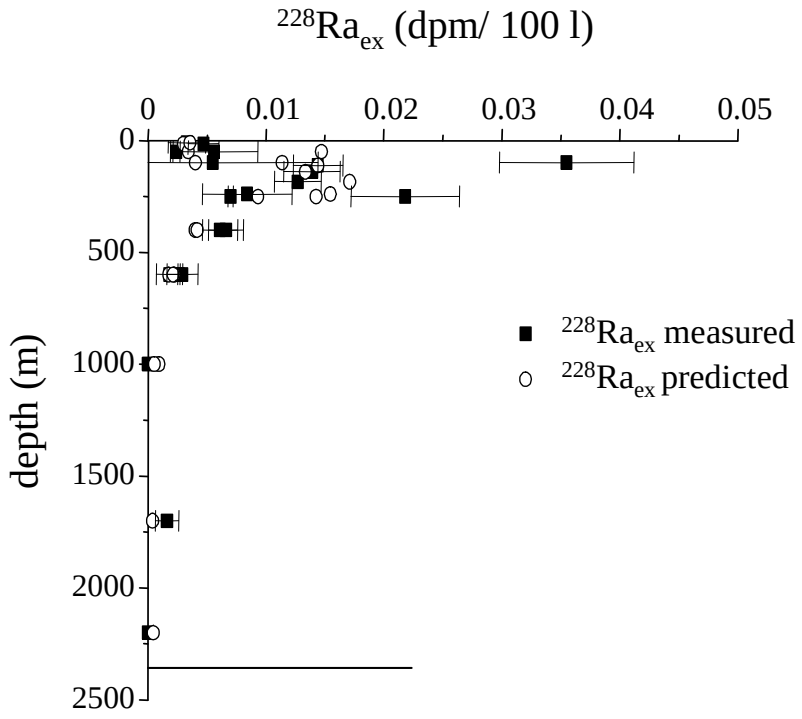

Figure 7 : $^{228}Ra_{ex}$ activities expected in suspended particles as deduced from the $^{226}Ra_{ex}$ activities measured in each sample and considering that the particles acquired the seawater $^{228}Ra/^{226}Ra$ ratio throughout the water column. Data acquired during all the BARMED cruises are reported on the same plot.

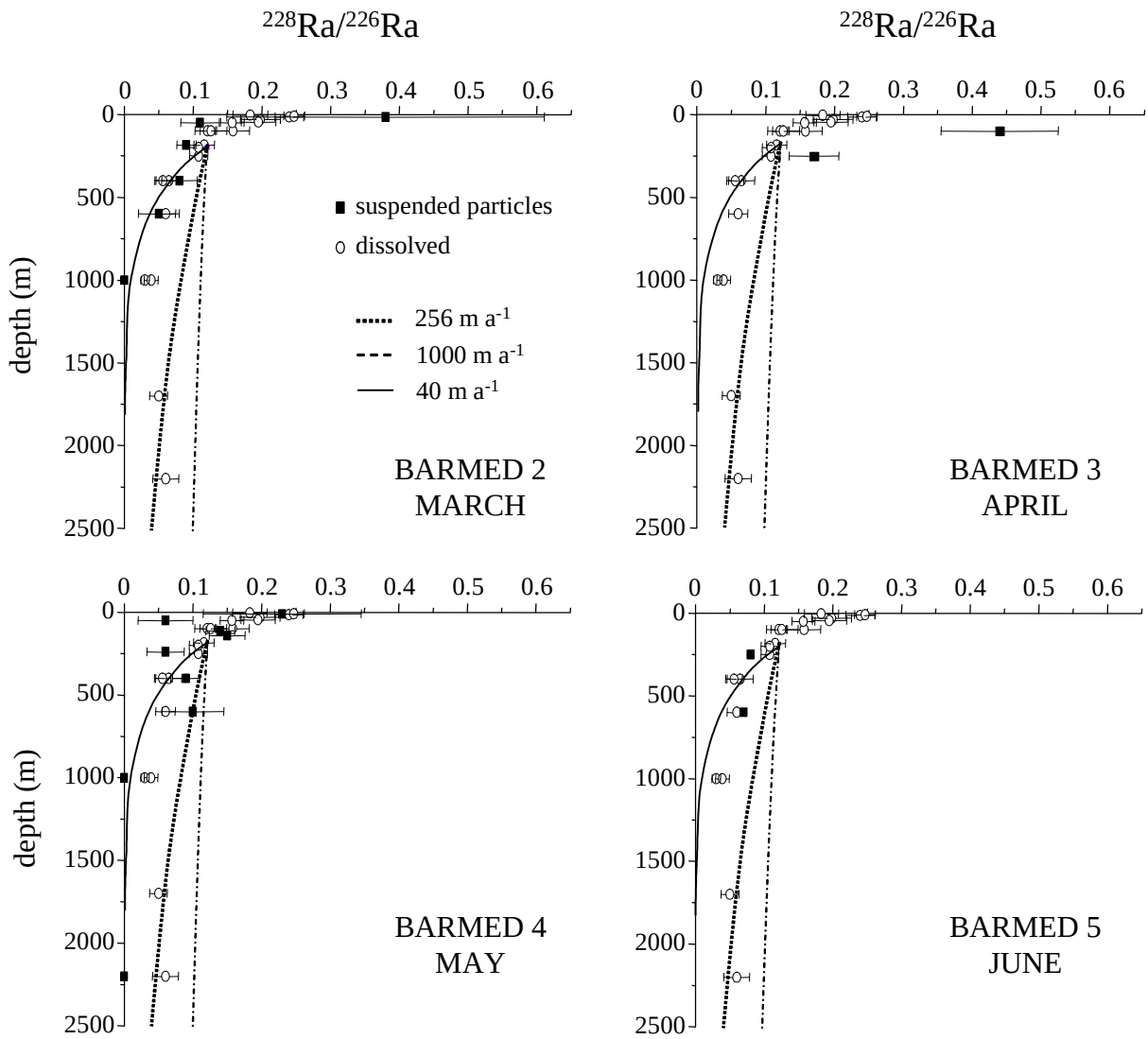

Figure 8 : $^{228}Ra_{ex}/^{226}Ra_{ex}$ ratio expected in suspended particles considering that the particles acquire the seawater ratio of subsurface waters (ratio of 0.12 at 200 m depth) and that they settle at speeds ranging from 256 m a^{-1} (Roy-Barman et al., 2002) to 1000 m a^{-1}. Ratios measured in the suspended particles associated with their error bars are shown in solid squares while the seawater ratios are shown in open circles.

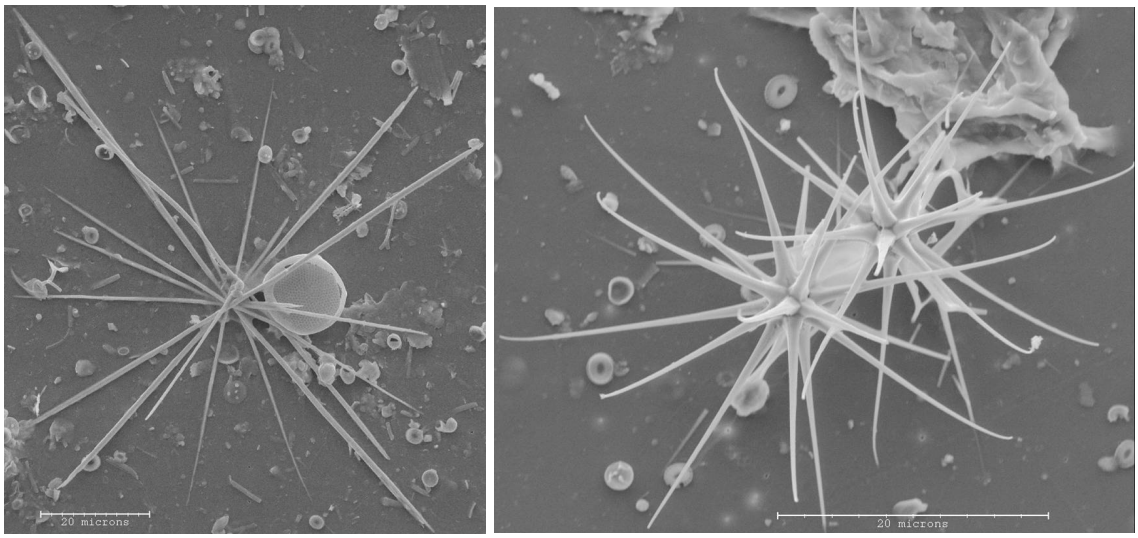

Figure 9 : SEM pictures of acantharian skeletons ($SrSO_4$) isolated from suspended particles collected at the DYFAMED site during the BARMED program.